Inorganic Chemistry

Article

Diligating Tripodal Amido-Phosphine Ligands: the Effect of a Proximal Antipodal Early Transition Metal on Phosphine Donor Ability in a Building Block for Heterometallic Complexes

Hua Han, Mona Elsmaili, and Samuel A. Johnson*

*Department of Chemistry and Biochemistry, University of Windsor, Windsor,
Ontario, Canada, N9B 3P4*

The ligand precursors $P(CH_2NH-3,5-(CF_3)_2C_6H_3)_3$ (**1a**), $P(CH_2NHPh)_3$ (**1b**), and $P(CH_2NH-3,5-Me_2C_6H_3)_3$ (**1c**), react with the reagents $Ti(NMe_2)_4$ and $^tBuN\!\!=\!\!Ta(NEt_2)_3$ to generate metal complexes of the type $P(CH_2NAr^R)_3TiNMe_2$ (**2a**–**c**) and $P(CH_2NAr^R)_3Ta\!\!=\!\!N^tBu$ (**3a**–**c**) (where $Ar^R = 3,5-(CF_3)_2C_6H_3$, Ph, and $3,5-Me_2C_6H_3$). Due to ring strain, the phosphine lone pair cannot chelate and is available to bind a second metal, and this feature can be utilized to synthesize heterometallic polynuclear complexes. The ^{31}P chemical shifts observed upon complexation of the early transition metals to the amido donors are large and in the opposite direction expected for the increased C–P–C bond angles in these complexes; these unusual shifts are due to P–Ti and P–Ta distances that are significantly shorter than the sum of van der Waals radii. The reaction of **2c** with $Ni(CO)_4$ produces at first the bimetallic complex $(CO)_3Ni[P(CH_2N-3,5-Me_2C_6H_3)_3TiNMe_2]$ (**4c**), which gradually converts to the trimetallic complex $(CO)_2Ni[P(CH_2N-3,5-Me_2C_6H_3)_3TiNMe_2]_2$ (**5c**). The effect of the complexation of Ti and Ta fragments on the donor ability of the phosphine ligand was determined by the preparation of the bis-phosphine complexes *trans*-L_2Rh-(CO)Cl, (where L = **1a**–**c**, **2a**–**c**, and **3a**–**c**) prepared by the reaction of the appropriate phosphine with $[Rh(CO)_2$-(μ-Cl)]_2$, and a measurement of the resultant CO stretching frequencies. Surprisingly, the complexes with the larger C–P–C angles are significantly poorer donors. Density functional theory calculations were performed to determine what factors affect the donor ability of the phosphine and if through-space interactions might play an important role in the observed electronic properties.

Introduction

The chemistry of polynuclear and heterobimetallic[1] clusters has been of interest to chemists[2] due to the ability of adjacent metals to cooperatively activate substrates. This is observed frequently in biological systems, where clusters of metals can assist in the transfer of electrons[3] to activate relatively inert substrates.[4] More recently, rational cluster synthesis has been used for the tuning of physical properties, such as single-molecule magnetism,[5] and early-late heterobimetallics have been used to synthesize unusual molecular architectures via self-assembly.[6]

We have recently shown that ligands of the type $P(CH_2-NAr^R)_3$, where Ar^R is an aryl substituent, can adopt a conformation where the phosphine and amido lone pairs are

---

* To whom correspondence should be addressed. E-mail: sjohnson@
uwindsor.ca. Fax: (519) 973-7098.

(1) Stephan, D. W. *Coord. Chem. Rev.* **1989**, *95*, 41–107. Wheatley, N.; Kalck, P. *Chem. Rev.* **1999**, *99*, 3379–3419.
(2) Braunstein, P.; Morise, X.; Benard, M.; Rohmer, M.-M.; Welter, R. *Chem. Commun.* **2003**, 610–611. Hernandez-Gruel, M. A. F.; Perez-Torrente, J. J.; Ciriano, M. A.; Rivas, A. B.; Lahoz, F. J.; Dobrinovitch, I. T.; Oro, L. A. *Organometallics* **2003**, *22*, 1237–1249. Kabashima, S.-i.; Kuwata, S.; Hidai, M. *J. Am. Chem. Soc.* **1999**, *121*, 7837–7845. Graham, T. W.; Llamazares, A.; McDonald, R.; Cowie, M. *Organometallics* **1999**, *18*, 3502–3510. Spannenberg, A.; Oberthur, M.; Noss, H.; Tillack, A.; Arndt, P.; Kempe, R. *Angew. Chem., Int. Ed.* **1998**, *37*, 2079–2082. Gade, L. H.; Schubart, M.; Findeis, B.; Fabre, S.; Bezougli, I.; Lutz, M.; Scowen, I. J.; McPartlin, M. *Inorg. Chem.* **1999**, *38*, 5282–5294.
(3) Gray, H. B.; Malmstroem, B. G. *Biochemistry* **1989**, *28*, 7499–7505.
(4) Messerschmidt, A.; Huber, R.; Wieghardt, K.; Poulos, T. *Handbook of Metalloproteins, Volume 1*; Wiley: New York, 2001.
(5) Christou, G.; Gatteschi, D.; Hendrickson, D. N.; Sessoli, R. *MRS Bull.* **2000**, *25*, 66–71. Gatteschi, D.; Sessoli, R. *Angew. Chem., Int. Ed.* **2003**, *42*, 268–297.
(6) Alvarez-Vergara, M. C.; Casado, M. A.; Martin, M. L.; Lahoz, F. J.; Oro, L. A.; Perez-Torrente, J. J. *Organometallics* **2005**, *24*, 5929–5936. Stang, P. J.; Persky, N. E. *Chem. Commun.* **1997**, 77–78. Mokuolu, Q. F.; Avent, A. G.; Hitchcock, P. B.; Love, J. B. *J. Chem. Soc., Dalton Trans.* **2001**, 2551–2553. Mokuolu, Q. F.; Duckmanton, P. A.; Hitchcock, P. B.; Wilson, C.; Blake, A. J.; Shukla, L.; Love, J. B. *Dalton Trans.* **2004**, 1960–1970.
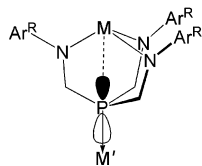
Figure 1. Potential binding mode of the of $P(CH_2NAr^R)_3$ ligands to an early transition metal fragment (shown as M) and a second metal complex (shown as M′) along with an illustration of the major and minor lobes of the lone pair orbital on phosphorus.

Figure 2. ORTEP depiction of the solid-state structure of **1a** as determined by X-ray crystallography. Selected bond angles: C(1)−P(1)−C(2), 99.48-(11); C(1)−P(1)−C(3), 99.38(15); C(2)−P(1)−C(3), 100.59(16); P(1)−C(1)−N(1), 107.99(18); P(1)−C(2)−N(2), 107.79(16); C(1)−N(1)−C(4), 123.7(2); C(2)−N(2)−C(12), 120.95(19).

arranged approximately parallel and are incapable of all chelating to the same metal; such a bonding mode was observed in a nonanuclear Cu(I) complex.[7] When M is a high-oxidation-state early transition metal, the bonding mode shown in Figure 1 is more likely, where the amido donors chelate to the early transition metal.[8] In this bonding mode, the phosphine ligand cannot bind its lone pair to the metal chelated by the amido donors but is well situated to bind to a second metal complex, labeled in Figure 1 as M′.

These ligands are thus well-suited for the facile synthesis of early−late transition metal heterobimetallic complexes, providing that some interaction between the two metal centers bound to either side of the ligand is possible. A direct through-space interaction between M and the minor lobe of the lone-pair orbital could allow for communciation between metal centers.[9] Such an interaction could mitigate the transfer of electrons between metals in complexes of these types or facilitate magnetic coupling between the metals in paramagnetic complexes. This paper describes an initial study on the ability of this ligand to cooordinate both early and late transition metals to prepare heterobimetallic and polynuclear complexes and an investigation of the role of the nature of the amido-chelated early transition metal on the properties of the phosphine donor.

Results and Discussion

Ligand Precursor Syntheses. The ligand precursors $P(CH_2NH-3,5-(CF_3)_2C_6H_3)_3$ (**1a**), $P(CH_2NHPh)_3$ (**1b**), and $P(CH_2NH-3,5-Me_2C_6H_3)$ (**1c**) were prepared using $P(CH_2-OH)_3$ with the appropriate aniline, as shown in Scheme 1. Although this reaction can be performed in toluene, with water removed by azeotropic distillation using a Dean−Stark apparatus, as previously reported for **1b**,[10] this requires the use of an excess (5 equiv) of aniline. We found it more convenient to perform the reaction neat and use dynamic vacuum to remove the byproduct, water. This procedure worked well with a stoichiometric amount of aniline, which simplified the purification procedure. The reaction occurred over 30 min and was exothermic. The product is analytically pure when prepared in this manner, though it is easily crystallized from a saturated warm toluene solution by cooling to −40 °C. A solvent-free procedure also worked
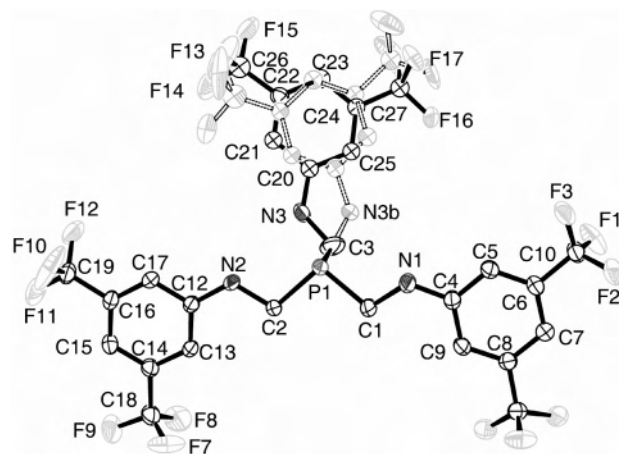
well using 3,5-dimethylaniline to produce **1c**; however, using 3,5-bis(trifluoromethyl)aniline no reaction was observed with the solvent-free methodology, and it was necessary use the original procedure using toluene as the solvent and a Dean−Stark apparatus to remove water to obtain **1a**. For simplicity, these ligand precursors will be abbreviated herein as [P(CH_2-NAr^R)]H_3, where Ar^R = 3,5-(CF_3)_2C_6H_3, Ph, and 3,5-Me_2C_6H_3, for **a**, **b**, and **c**, respectively. Ligand precursors **1a**−**c** oxidize only slowly in air and are not particularly moisture sensitive, although they were stored under a dry nitrogen atmosphere.

Scheme 1
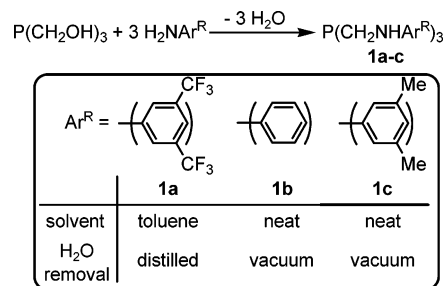
Compounds **1b** and **1c** both crystallized as thin plates unsuitable for crystallographic studies; however, crystals of **1a** suitable for X-ray diffraction were obtained by slow evaporation of a toluene solution. An ORTEP depiction of the solid-state structure obtained at 133 K is shown in Figure 2. Unfortunately, this structure suffers slightly from disorder of one of the ligand arms and rotational disorder of a majority of the CF_3 substituents. The C(1)−P(1)−C(2), C(1)−P(1)−C(3), and C(2)−P(1)−C(3) angles for the free ligand precursor **1c** are 99.48(11)°, 99.38(15)°, and 100.59(16)°, respectively, for a sum of 299.5(2)°; this value is fairly typical for phosphine donors, whose C−P−C angles are invariably much less than the tetrahedral angle of 109.5°. This change in sum of C−P−C angles will be used to evaluate the effects of complexation of early transition metals to the amido donors on the phosphine donor (vide infra).

(7) Keen, A. L.; Doster, M.; Han, H.; Johnson, S. A. *Chem. Commun.* **2006**, 1221−1223.

(8) Gade, L. H. *Acc. Chem. Res.* **2002**, *35*, 575−582; Gade, L. H. *J. Organomet. Chem.* **2002**, *661*, 85−94. Jia, L.; Ding, E.; Rheingold, A. L.; Rhatigan, B. *Organometallics* **2000**, *19*, 963−965.

(9) Hoffmann, R. *Acc. Chem. Res.* **1971**, *4*, 1−9.

(10) Frank, A. W.; Drake, G. L., Jr. *J. Org. Chem.* **1972**, *37*, 2752−2755.
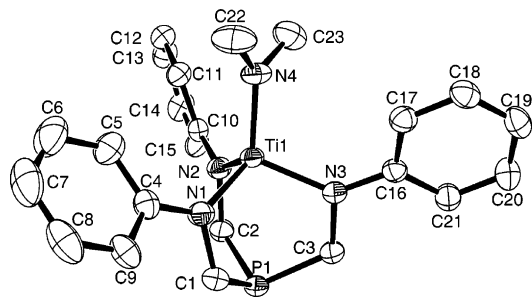
Figure 3. Solid-state molecular structure of **2b** as determined by X-ray crystallography. Hydrogen atoms are omitted for clarity. Selected distances (Å): Ti(1)···P(1), 2.9895(4); Ti(1)−N(1), 1.9239(11); Ti(1)−N(2), 1.9327-(11); Ti(1)−N(3), 1.9424(11); Ti(1)−N(4), 1.8643(12). Selected bond angles: C(1)−P(1)−C(2), 105.85(6); C(1)−P(1)−C(3), 102.64(6); C(2)−P(1)−C(3), 102.89(6); Ti(1)−N(4)−C(22), 130.95(11); Ti(1)−N(4)−C(23), 115.22(10); Ti(1)−N(1)−C(1), 109.48(8); Ti(1)−N(1)−C(4), 132.54(9); Ti-(1)−N(2)−C(2), 108.78(8); Ti(1)−N(2)−C(10), 133.75(9); Ti(1)−N(3)−C(3), 109.80(8); Ti(1)−N(3)−C(16), 134.33(9); P(1)−C(1)−N(1), 116.64-(9); P(1)−C(2)−N(2), 118.59(9); P(1)−C(3)−N(3); 117.06(9); C(1)−N(1)−C(4), 117.13(11); C(2)−N(2)−C(10), 117.47(11); C(3)−N(3)−C(16), 115.74(10).

Titanium Complex Syntheses. The reactions of **1a−c** with Ti(NMe$_2$)$_4$ in toluene produce P(CH$_2$NAr^R)$_3$TiNMe$_2$, **2a−c**, as shown in eq 1. These reactions are slow at room temperature and require 12−24 h to go to completion. No intermediates were observed by ^{1}H or ^{31}P{^{1}H} NMR spectroscopy. The resultant products are all obtained in high yields as thermally stable dark-red crystalline solids.

$$ \text{P(CH}_2\text{NHAr}^R)_3 + \text{Ti(NMe}_2)_4 \xrightarrow[-3\ \text{HNMe}_2]{\text{toluene}} \quad (1) $$
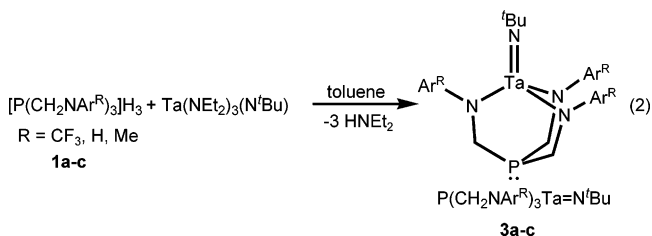
P(CH$_2$NAr^R)$_3$TiNMe$_2$

2a-c
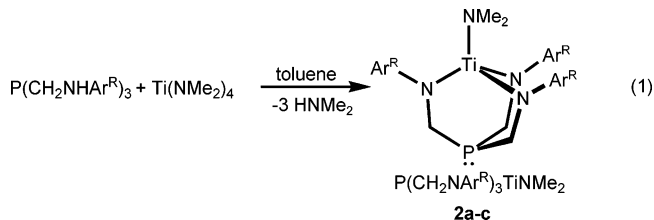
The solid-state structures of **2a−c** were determined by X-ray crystallography. An ORTEP depiction of the solid-state molecular structure of **2b** is shown in Figure 3; a comparison of the bond lengths and angles with those of **2a** and **2c** revealed little variation, although the quality of the structure of **2c** was hampered by the tendency of this compound to crystallize as nonmerohedral twins. The structural data for **2a** and **2c** are contained in the Supporting Information. As anticipated, in all three structures, the tripodal ligand chelates via three amido donors and the lone-pair of the phosphine donor is directed away from the metal center.

A comparison of the C−P−C angles before and after the introduction of a transition metal to the triamido chelate provides some measure of the hybridization change at the phosphine donor, which should affect its donor properties. In **2b**, the sum of C−P−C angles is 311.4(1)° compared to 299.5(2)° in **1a**, which is a significant change. Although the phosphine donor is hybridized so that the lone pair is formally directed away from the early transition metal, the binding of the ligand enforces P···Ti distances that are under the sum of van der Waals radii of these elements.[11] For **2b**, the P···Ti distance of 2.9895(4) Å for **2b** is only ∼6% larger

(11) Bondi, A. *J. Phys. Chem.* **1964**, *68*, 441−451.

than the longest reported phosphine−titanium bond length of 2.813 Å,[12] although Ti−P bond distances are more typically 2.6−2.7 Å.

Despite the fact that the phosphine lone pair is not coordinated to the early transition metal center, the ^{31}P{^{1}H} NMR shifts are strongly affected by the coordination of a transition metal to the amido donors. A small range of chemical shifts are observed for the free ligands by ^{31}P{^{1}H} NMR spectroscopy: δ −32.6, −31.0, and −29.6 for **1a−c**, respectively. In **2a−c**, both the shifts and the range covered are vastly different, with shifts of δ −79.9, −65.6, and −61.6 for **2a−c**, respectively. The change of the chemical shift to higher field for **2a−c** compared to their ligand precursors was unexpected; an increase in C−P−C angle usually leads to a significant shift to lower field. For example, the opposite trend of chemical shifts vs C−P−C angle is observed for the alkyl phosphines PMe$_3$, PEt$_3$, and P^{t}Bu$_3$, whose ^{31}P shifts are δ −62, −20, and +63, respectively. The modeling of ^{31}P NMR shifts is complex;[13] however, these results indicate that the phosphorus donor may be directly affected by its proximity to the chelated early transition metal.

Tantalum Complex Syntheses. The reaction of **1a−c** with Ta(NEt$_2$)$_3$(N^{t}Bu) cleanly produced the tantalum imido complexes P(CH$_2$NAr^R)$_3$Ta=N^{t}Bu, **3a−c**, as shown in eq 2. The products were obtained in high yields as yellow crystalline solids. As with **2a−c**, the ^{1}H NMR spectra of **3a−c** are consistent with apparent C_{3v} symmetry.

$$ [\text{P(CH}_2\text{NAr}^R)_3]\text{H}_3 + \text{Ta(NEt}_2)_3(\text{N}^t\text{Bu}) \xrightarrow[-3\ \text{HNEt}_2]{\text{toluene}} \quad (2) $$

R = CF$_3$, H, Me

1a-c

P(CH$_2$NAr^R)$_3$Ta=N^{t}Bu

3a-c

The solid-state structure of **3b** was determined by X-ray crystallography, and an ORTEP depiction of the solid-state molecular structure of **3b** is shown in Figure 4. As with complexes **2a−c**, the triamido donors chelate to the early transition metal, and the phosphine lone pair is directed away from the Ta center. The C−P−C angles for **3b** are larger than those of the titanium complexes **2a−c**, with a sum of C−P−C angles of 315.0(2)°. Clearly, the chelation of a metal requires an increase in the bond angles at P, with the greater increase for the larger metal, Ta. This difference is more than expected, considering the relatively small difference between the size of Ti and Ta. Despite the slightly larger size of Ta, the P···Ta distance in **3b** is 2.9548(6) Å, which is shorter than the P···Ti distance in **2b**, and only 3.5% longer than the longest reported phosphine−tantalum bond length of 2.855 Å.[14]

The change in ^{31}P NMR shifts of **1a−c** upon coordination of the amido donors to tantalum are more dramatic than those
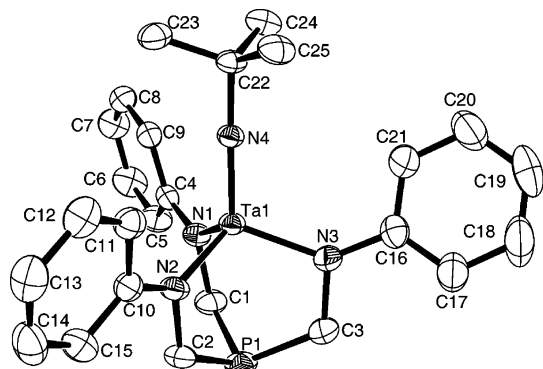
(12) Shao, M.-Y.; Gau, H.-M. *Organometallics* **1998**, *17*, 4822−4827.
(13) Feindel, K. W.; Wasylishen, R. E. *Can. J. Chem.* **2004**, *82*, 27−44.
(14) van Doorn, J. A.; van der Heijden, H.; Orpen, A. G. *Organometallics* **1994**, *13*, 4271−4277.

Figure 4. Solid-state molecular structure of **3b** as determined by X-ray crystallography. Hydrogen atoms are omitted for clarity. Selected distances (Å): Ta(1)···P(1), 2.9548(6); Ta(1)−N(1), 2.004(2); Ta(1)−N(2), 1.998-(2); Ta(1)−N(3), 1.990(2); Ta(1)−N(4), 1.7682(18). Selected bond angles in degrees: C(1)−P(1)−C(2), 103.91(13); C(1)−P(1)−C(3), 105.77(12); C(2)−P(1)−C(3), 105.27(12); Ta(1)−N(1)−C(1), 105.77(15); Ta(1)−N(1)−C(4), 137.42(15); C(1)−N(1)−C(4), 116.8(2); Ta(1)−N(2)−C(2), 105.27-(15); Ta(1)−N(2)−C(10), 138.42(16); C(2)−N(2)−C(10), 116.3(2); Ta(1)−N(3)−C(16), 135.96(17).

observed for titanium, though the range of observed shifts is smaller, with shifts of δ −108.5, −100.9, and −100.1 for complexes **3a**−**c**, respectively. Contrary to what might be expected, the trend of phosphorus shifts for the free ligand, Ti, and Ta complexes seem to indicate that the phosphine donors are becoming poorer donors with increasing C−P−C angle; however, it is difficult to be certain that the changes in chemical shift truly represent a reduced donor ability of the phosphine donor.

Characterization of the Phosphine Donor. The standard measures of a phosphine donor are its electronic parameter, usually obtained from the symmetric CO stretching frequency of a carbonyl complex of the phosphine,[15] and the cone angle, as defined by Tolman with respect to Ni(CO)$_3$ complexes.[16] Although numerous other approaches have been described, most still attempt to classify the properties of a phosphine in terms of steric[17−19] and electronic effects.[20] From the structure of the titanium complex **2b**, the cone angle of the phosphine donor can be estimated as 100° if the methylene hydrogens are used to define the cone angle, where the hydrogen atom is given a radius of 0.6 Å, and a metal−P distance of 2.28 Å is assumed, as described by Tolman. For the tantalum complex **3b**, the estimated cone angle is 103°, which is larger due to the increase in C−P−C angles relative to the titanium complexes. For **2a** and **2c**, the trifluoromethyl or methyl meta substituents define the cone angle, rather than the methylene hydrogens, which makes these complexes

slightly larger donors, although realistically the aryl groups can probably rotate so that cone angles predicted from the location of these substituents overestimate the size of these donors. Regardless, these complexes display remarkably small cone angles, which are comparable to those of the smallest of phosphine donors. For comparison, the cone angles of PMe$_3$, PEt$_3$, PPh$_3$, and P(OEt)$_3$ are all larger, at 118°, 132°, 145°, and 109°, respectively.
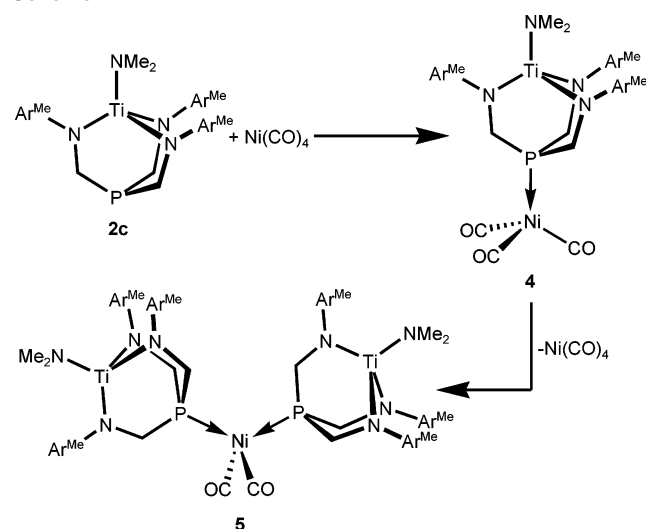
The electronic properties of many phosphines have been characterized by measurement of the A_1 stretching frequency of complexes prepared by replacement of a CO group in Ni(CO)$_4$ by a single phosphine donor. Less-toxic compounds than Ni(CO)$_4$ are now more commonly used to characterize the electronic properties of phosphines; however, we opted to prepare a complex of Ni(CO)$_4$ to have a chance to compare the parameters of some of these phosphine complexes directly with large database of data available for adducts of the Ni(CO)$_3$ moiety. Compound **2c** reacted instantaneously with excess Ni(CO)$_4$ to afford, at first, a single product, which was determined to be (CO)$_3$Ni[P(CH$_2$NAr^{Me})$_3$]-TiNMe$_2$, **4**, as assessed by ^{1}H, ^{13}C{^{1}H}, and ^{31}P{^{1}H} NMR spectroscopy. The coordination of phosphorus to nickel is accompanied by a large ^{31}P{^{1}H} NMR shift from δ −61.6 in **2c** to δ +4.1,[21] and the ^{13}C{^{1}H} carbonyl carbon resonance at δ 196.3, which is a doublet with a typical $^2J_{PC}$ value of 1.1 Hz,[22] confirms the coordination of a single phosphine donor. The symmetric A_1 carbonyl stretching frequency of a 0.05 mol L^{-1} solution of (CO)$_3$Ni[P{CH$_2$N(C$_6$H$_3$R$_2$)}$_3$-TiNMe$_2$] in CH$_2$Cl$_2$ was 2073.7 cm^{-1}; this can be compared to the extensive data tabulated by Tolman.[16] Compared to other phosphine ligands, P(CH$_2$NAr^R)$_3$]TiNMe$_2$ is significantly less strongly electron-donating than the common alkyl phosphines PMe$_3$ ($\upsilon_{CO}(A_1)$ = 2064.1 cm^{-1}), and slightly less electron donating than the ubiquitous PPh$_3$ ($\upsilon_{CO}(A_1)$ = 2068.9 cm^{-1}). The electronic parameter for **4** is almost identical to PHPh$_2$ ($\upsilon_{CO}(A_1)$ = 2073.3 cm^{-1}). As a phosphine ligand, complex **4** appears to be a capable π-acceptor but not as strong a π-acid as typical phosphites, such as P(OEt)$_3$ ($\upsilon_{CO}(A_1)$ = 2076.3 cm^{-1}).

Compound **4** is not stable at room temperature, and solutions undergo ligand redistribution over the course of 48 h to form over 50% (CO)$_2$Ni[P(CH$_2$NAr^{Me})$_3$TiNMe$_2$]$_2$, **5**, presumably with loss of Ni(CO)$_4$. This reaction sequence is depicted in Scheme 2. The ^{31}P{^{1}H} NMR spectrum shows an additional peak at δ 7.0, and the ^{13}C{^{1}H} NMR carbonyl resonance is a triplet at δ 190.0 due to coupling to two identical phosphorus nuclei. The resonance for the methylene carbon, which is typically a doublet due to a $^1J_{PC}$ of around 15 Hz, in this case is a virtual triplet due to the AA′XX′ spin system. Further ligand redistribution appears to occur as the conversion to **5** increases and results in the formation of an impurity, which is presumably the trisubstituted complex; this makes the high-yield isolation of pure **5** by this procedure difficult. Addition of an equivalent of **2b** to

(15) Strohmeier, W.; Mueller, F. J. *Chem. Ber.* **1967**, *100*, 2812−2821. Tolman, C. A. *J. Am. Chem. Soc.* **1970**, *92*, 2953−2956.
(16) Tolman, C. A. *Chem. Rev.* **1977**, *77*, 313−348.
(17) Bunten, K. A.; Chen, L.; Fernandez, A. L.; Poe, A. J. *Coord. Chem. Rev.* **2002**, *233−234*, 41−51. Ferguson, G.; Roberts, P. J.; Alyea, E. C.; Khan, M. *Inorg. Chem.* **1978**, *17*, 2965−2967.
(18) Cooney Katharine, D.; Cundari Thomas, R.; Hoffman Norris, W.; Pittard Karl, A.; Temple, M. D.; Zhao, Y. *J. Am. Chem. Soc.* **2003**, *125*, 4318−4324.
(19) Dunne, B. J.; Morris, R. B.; Orpen, A. G. *J. Chem. Soc., Dalton Trans.* **1991**, 653−661.
(20) Rahman, M. M.; Liu, H. Y.; Eriks, K.; Prock, A.; Giering, W. P. *Organometallics* **1989**, *8*, 1−7. Bush, R. C.; Angelici, R. J. *Inorg. Chem.* **1988**, *27*, 681−686. Suresh, C. H.; Koga, N. *Inorg. Chem.* **2002**, *41*, 1573−1578.

(21) Mathieu, R.; Lenzi, M.; Poilblanc, R. *Inorg. Chem.* **1970**, *9*, 2030−2034.
(22) Bodner, G. M.; May, M. P.; McKinney, L. E. *Inorg. Chem.* **1980**, *19*, 1951−1958.
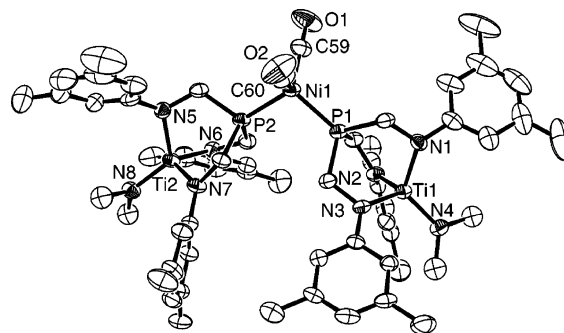
Scheme 2

Figure 5. ORTEP depiction of the solid-state molecular structure of $(CO)_2Ni[P(CH_2N\text{-}3,5\text{-}Me_2C_6H_3)_3TiNMe_2]_2$ (**5**). Hydrogen atoms are omitted for clarity. Selected distances (Å): P(1)−Ni(1), 2.1835(13); P(2)−Ni(1), 2.1900(14); Ti(1)···P(1), 3.087(5); Ti(2)···P(2), 3.097(5); N(1)−Ti(1), 1.938(4); N(2)−Ti(1), 1.942(4); N(3)−Ti(1), 1.922(4); N(4)−Ti(1), 1.872-(4); N(5)−Ti(2), 1.943(4); N(6)−Ti(2), 1.937(4); N(7)−Ti(2), 1.923(4); N(8)−Ti(2), 1.857(4). Selected angles in degrees: P(1)−Ni(1)−P(2), 104.00(5); C(59)−Ni(1)−C(60), 111.4(2); P(1)−Ni(1)−C(59), 111.22(19); P(1)−N(1)−C(60), 109.96(17); P(2)−Ni(1)−C(59), 110.98(16); P(2)−Ni-(1)−C(60) 108.97(19); C(1)−P(1)−C(2), 102.4(2); C(2)−P(1)−C(3), 103.7-(2); C(3)−P(1)−C(1), 101.4(2); C(30)−P(2)−C(31), 101.3(2); C(31)−P(2)−C(32), 103.6(2); C(30)−P(2)−C(32), 101.5(2); C(1)−P(1)−Ni(1), 116.31(14); C(2)−P(1)−Ni(1), 116.34(15); C(3)−P(1)−Ni(1), 114.66(15); C(30)−P(2)−Ni(1), 114.98(14); C(31)−P(2)−Ni(1), 117.10(16); C(32)−P(2)−Ni(1), 116.09(15).

a freshly prepared sample of **4** proved to be the most effective synthesis of **5**.

The molecular structure of **5** was determined by single-crystal X-ray crystallography and is shown in Figure 5. The bonding of the phosphine donor to nickel appears to have some effects on the structure of the ligand. The Ti(1)···P(1) and Ti(2)···P(2) short contacts are 3.087(5) and 3.097(5) Å, respectively, whereas in **2c**, a Ti···P distance of 3.015(5) Å was observed, a difference of 0.08(1) Å. The sum of C−P−C angles for P(1) and P(2) are 307.5(3)° and 306.4(3)°, respectively, which is a slight decrease from 310.5(5)° in **2c**. This result is quite unusual because the coordination of phosphine donors to metal centers almost invariably results in an increase of C−P−C angles by 3° or 4°, even in related cyclic systems such as P(CH_2O)_3P; this effect is often explained by the simple application of VSEPR theory. Although the absence of an increase in C−P−C angles could be explained by the initial strain on the ligand to accommodate the large Ti metal center, the decrease in C−P−C angle upon coordination to Ni is not easy to rationalize. This compression of C−P−C angles has a considerable effect on the geometry at Ti. The sum of the N(1)−Ti(1)−N(2), N(2)−Ti(1)−N(3), and N(1)−Ti(1)−N(3) angles decreases from 316.4(1)° in **2b** to 304.0(3)° in **5**, both of which deviate considerably from the 328.5° expected for a tetrahedral structure.

Another method to assess the steric bulk of a phosphine is the symmetric deformation coordinate, which is defined as the difference between the sum of these C−P−C and Ni−P−C angles.[19] In **5**, the sum of Ni(1)−P−C angles for P(1) and P(2) is 347.3(3)° and 348.2(3)°, respectively, which results in symmetric deformation coordinates of 39.8(4)° and 41.8(4)° for P(1) and P(2), respectively. As with the cone angle, these values are indicative of a small donor.

Examination of the geometry at Ni(1) in the structure of **5** reveals a few points worthy of mention. The P(1)−Ni(1) and P(2)−Ni(1) distances are 2.1835(13) and 2.1900(14) Å, respectively, which is approximately 0.1 Å shorter than the average phosphine−nickel bond length of 2.28 Å. A direct measurement of the cone angle of these ligands yields a value

of 106°, a value larger than we estimated from the structure of **2b**; however, this increase is entirely due to the shorter than average Ni−P bond length. The diminutive nature of these phosphines is apparent from the P(1)−Ni(1)−P(2) angle of 104.00(5)°, which is significantly smaller than the tetrahedral angle of 109.5°.

Phosphine Electronic Parameters from Reactions with [Rh(CO)_2(μ-Cl)]_2. The addition of 4 equiv of most phosphine donors to [Rh(CO)_2(μ-Cl)]_2 allows for the facile preparation of *trans*-rhodiumcarbonylchlorobisphosphine complexes, and the CO stretching frequency of these adducts have been used extensively in the past to determine electronic parameters for phosphine ligands. To avoid the repeated handling of highly toxic Ni(CO)_4, we chose to evaluate the electronic properties of the phosphine donor in **1a−c**, **2a−c**, and **3a−c** by this method. ^{1}H and ^{31}P{^{1}H} NMR spectroscopy was used to identify the products as the *trans*-rhodiumcarbonylchlorobisphosphine complexes **6a−c**, **7a−c**, and **8a−c** of the phosphines **1a−c**, **2a−c**, and **3a−c**, respectively, as shown in Scheme 3. The products were all formed within 20 min of dissolving the reagents in CH_2Cl_2.

The adduct of **3c**, *trans*-Cl(CO)Rh[P(CH_2NAr^{Me})_3Ta═N^{t}Bu]_2 (**8c**) was isolated and characterized by X-ray crystallography. The solid-state molecular structure of **8c** is shown in Figure 6. The crystallographically imposed symmetry in the structure of **8c** is C_{3h}, which leads to a 3-fold disorder of the carbonyl and chloride ligands; only one location is shown in Figure 6. In a projection along the P−Rh−P 3-fold axis, the larger Cl ligand is staggered with respect to the P−CH_2 bonds, whereas the smaller carbonyl ligand is eclipsed. The sum of C−P−C angles is 319.0(3)°, which is approximately 4° larger than the sum of C−P−C angles in **3b**; this increase in C−P−C angle is typical for the coordination of phosphine to metal centers, unlike the decrease of C−P−C angle noted previously for complex **5**.
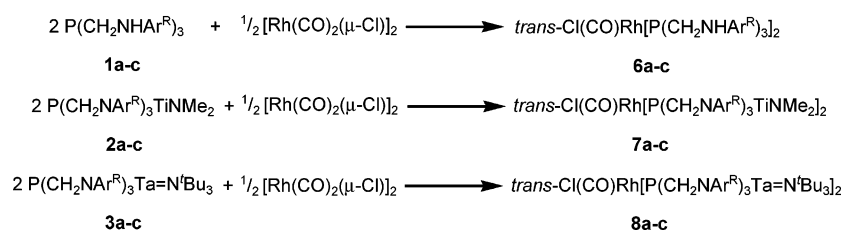
Scheme 3

$$2\ P(CH_2NHAr^R)_3\quad +\quad {}^1\!/_2\,[Rh(CO)_2(\mu\text{-Cl})]_2\ \longrightarrow\ \textit{trans-}Cl(CO)Rh[P(CH_2NHAr^R)_3]_2$$

$$\mathbf{1a\text{-}c}\qquad\qquad\qquad\qquad\qquad\qquad\qquad\qquad\qquad\mathbf{6a\text{-}c}$$

$$2\ P(CH_2NAr^R)_3TiNMe_2\ +\ {}^1\!/_2\,[Rh(CO)_2(\mu\text{-Cl})]_2\ \longrightarrow\ \textit{trans-}Cl(CO)Rh[P(CH_2NAr^R)_3TiNMe_2]_2$$

$$\mathbf{2a\text{-}c}\qquad\qquad\qquad\qquad\qquad\qquad\qquad\qquad\qquad\mathbf{7a\text{-}c}$$

$$2\ P(CH_2NAr^R)_3Ta{=}N^tBu_3\ +\ {}^1\!/_2\,[Rh(CO)_2(\mu\text{-Cl})]_2\ \longrightarrow\ \textit{trans-}Cl(CO)Rh[P(CH_2NAr^R)_3Ta{=}N^tBu_3]_2$$

$$\mathbf{3a\text{-}c}\qquad\qquad\qquad\qquad\qquad\qquad\qquad\qquad\qquad\mathbf{8a\text{-}c}$$

Table 1. Crystallographic Data for Compounds **1a**, **2b**, **3b**, **5**, and **8c**

	1a	2b	3b
empirical formula	$C_{27}H_{18}F_{18}N_3P$	$C_{23}H_{27}N_4PTi$	$C_{25}H_{30}N_4PTa$
formula weight	757.41	438.33	598.45
crystal system	orthorhombic	monoclinic	monoclinic
a, Å	15.620(2)	11.9600(8)	27.980(3)
b, Å	16.410(2) Å	14.4825(9)	11.7166(12)
c, Å	22.386(3)	12.8136(8)	19.371(2)
α, deg	90.0	90.0	90.0
β, deg	90.0	90.081(1)	131.3410(10)
γ, deg	90.0	90.0	90.0
V, Å³	5738.0(13)	2219.45(2)	4767.9(8)
space group	$Pbca$ (No. 61)	$P2_1/n$	$C2/c$
Z value	8	4	8
μ(Mo Kα)	0.239 mm⁻¹	0.474 mm⁻¹	4.697 mm⁻¹
T	133 K	173 K	173 K
total no. of reflns	61 351	17 442	26 207
no. of unique reflns	6569 (R_{int} = 0.0282)	3903 (R_{int} = 0.019)	5417 (R_{int} = 0.021)
residuals: R1; wR2 (all data)	0.077; 0.187	0.034; 0.090	0.022; 0.046
	5	**8c**	
empirical formula	$C_{65}H_{90}N_8NiO_2P_2Ti_2$	$C_{63}H_{84}ClN_8OP_2RhTa_2$	
formula weight	1231.90	1531.58	
crystal system	triclinic	hexagonal	
a, Å	15.417(3)	14.2228(8)	
b, Å	15.812(3)	14.2228(8)	
c, Å	16.336(3)	25.594(3)	
α, deg	111.303(2)	90.0	
β, deg	109.839(2)	90.0	
γ, deg	95.691(2)	120.0	
V, Å³	3375.6(11)	4483.7(6)	
space group	$P\bar{1}$	$P6_3/m$ (No. 176)	
Z value	2	2	
μ(Mo Kα)	0.601 mm⁻¹	2.714 mm⁻¹	
T	173 K	173 K	
total no. of reflns	32 235	49 687	
no. of unique reflns	11 867 (R_{int} = 0.069)	3513 (R_{int} = 0.0429)	
residuals: R1; wR2 (all data)	0.109; 0.174	0.056; 0.1254	

As a result, the tantalum center moves further into the chelating amides compared to the structure of **3b** and the P(1)···Ta(1) distance of 2.943(2) Å is 0.012(2) Å shorter than in **3b**, as might be expected considering the larger
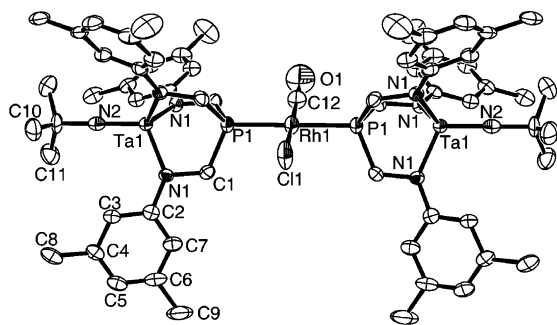

Figure 6. ORTEP depiction of the solid-state molecular structure of **8c** as determined by X-ray crystallography. Only one pair of the three disordered sites of occupancy of the Cl and CO ligands is shown, and hydrogen atoms are omitted for clarity. Selected distances (Å): P(1)···Ta-(1), 2.943(2); N(1)−Ta(1), 1.995(4); N(2)−Ta(1), 1.787(9); P(1)−Rh(1), 2.292(2). Selected bond angles: C(1)−P(1)−C(1), 106.33(19); Rh(1)−P(1)−C(1), 112.46(17).

C−P−C angles. The P(1)···Ta(1) distance in **8c** is only 3.0% longer than the longest crystallographically characterized tantalum−phosphine bonding interaction.[14] The sum of Rh−P−C angles is 337.4(3)°, which leads to a symmetric deformation coordinate of 18.4(4)°, which is less than half the value observed in the titanium−nickel complex, **5**.

The CO stretching frequencies of CH$_2$Cl$_2$ solutions of **6a−c**, **7a−c**, and **8a−c** are presented in Table 2 and plotted versus the ³¹P chemical shifts of the precursors **1a−c**, **2a−c**, and **3a−c** in Figure 7. It is clear from this chart that the effect of the different aryl substituents is very significant even for the ligand precursor complexes **6a−c**, despite the distance of these substituents from the phosphine donor. Such an influence demonstrates that the lone pairs on the nitrogen atoms are important in determining the electronic properties of these donors even in the absence of a transition metal. There is evidence for a preferential orientation of the nitrogen lone pairs with respect to both the aromatic ring substituents and the phosphine donor in the structure of **1c**, shown in Figure 2; the two ligand arms associated with N(1) and N(2)

Table 2. Metal Carbonyl Stretching Frequencies of Compounds **6a−c**, **7a−c** and **8a−c** in CH₂Cl₂, Their $^1J_{RhP}$ Coupling Constants and ^{31}P NMR Shifts, and the ^{31}P NMR Shifts of the Phosphine Donors **1a−c**, **2a−c**, and **3a−c**

Rh(I) complex	phosphine donors	ν_{CO} (cm^{-1})	$^1J_{Rh-P}$	coordinated ^{31}P shift	ligand ^{31}P shift
6a	P(CH₂NHAr^{CF_3})₃	1984.9	120.1	+22.6	−32.6 (**1a**)
6b	P(CH₂NHPh)₃	1976.3	118.1	+23.7	−31.0 (**1b**)
6c	P(CH₂NHAr^{Me})₃	1973.2	116.9	+23.5	−29.6 (**1c**)
7a	P(CH₂NAr^{CF_3})₃TiNMe₂	1988.0	130.3	+3.8	−79.9 (**2a**)
7b	P(CH₂NPh)₃TiNMe₂	1979.5	125.8	+15.7	−65.6 (**2b**)
7c	P(CH₂NAr^{Me})₃TiNMe₂	1975.3	122.5	+18.5	−61.6 (**2c**)
8a	P(CH₂NAr^{CF_3})₃Ta=NC(CH₃)₃	1990.5	143.6	−34.2	−108.5 (**3a**)
8b	P(CH₂NPh)₃Ta=NC(CH₃)₃	1986.7	138.1	−32.8	−100.9 (**3b**)
8c	P(CH₂NAr^{Me})₃Ta=NC(CH₃)₃	1986.6	136.9	−32.3	−100.1 (**3c**)
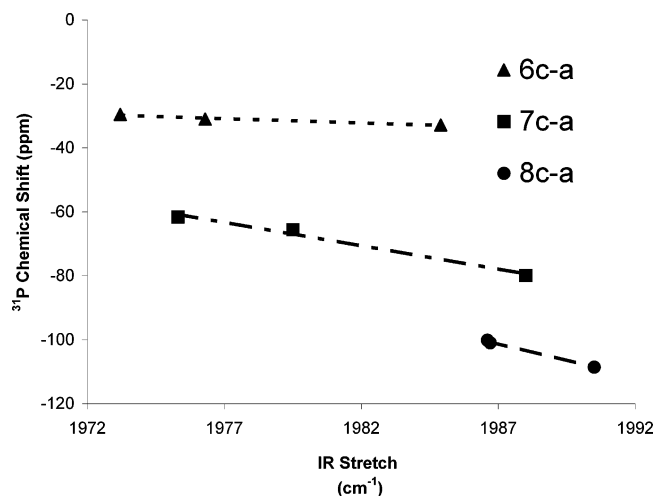
Figure 7. ^{31}P NMR chemical shift vs carbonyl stretching frequencies for complexes **6a−c**, **7a−c**, and **8a−c**.

are aligned so that their aromatic substituents, C(1), C(2), and P(1) are nearly coplanar. The effect of the aryl substituents is also apparent in the CO stretching frequencies of the titanium complexes, **7a−c**. The effect of the aryl substituents for these titanium complexes is practically identical to that observed for **6a−c**, although the titanium complexes are nearly uniformly less strongly donating than **6a−c**. In contrast, the CO stretches for the tantalum complexes **8a−c** are much less affected by the aryl substituents. The range of CO stretching frequencies for **8a−c** spans only 3.8 cm^{-1} for the three different aryl substituents, whereas for **6a−c** and **7a−c**, the ranges spanned are 11.7 and 12.7 cm^{-1}, respectively. Complexes **8b** and **8c** have nearly identical CO stretching frequencies. There is a near-linear trend to decreasing ^{31}P chemical shift with the decreasing donor ability of the phosphine for each set of complexes, **6a−c**, **7a−c**, and **8a−c**. Between sets of complexes, there is no linear trend between chemical shift and donor ability; however, the highest-field ^{31}P NMR chemical shifts do correlate with the weaker σ-donating phosphines. The most strongly donating phosphine ligands, **1b−c** and **2b−c**, have similar donor properties to PPh₃, which exhibits a CO stretching frequency of 1978 cm^{-1} in the complex *trans*-Rh(CO)Cl(PPh₃)₂.

Table 2 also contains the ^{31}P NMR shifts and $^1J_{RhP}$ values for complexes **6a−c**, **7a−c**, and **8a−c**, along with the ^{31}P NMR shifts of the phosphine donors **1a−c**, **2a−c**, and **3a−c**. For complexes **6a−c**, the $^1J_{RhP}$ values ranges from 116.9

to 120.1 Hz, with the largest values for **6a**, which bears the most electron-withdrawing substituents. An increase in phosphine lone pair s-orbital character is consistent with the poorer donor ability of this phosphine, although many factors can affect Rh−P coupling constants.[16] The same trend is observed for complexes **7a−c**, and the poorer donor abilities of these phosphines relative to **6a−c** are consistent with their larger $^1J_{RhP}$ values, which range from 122.5 to 130.3 Hz. For the tantalum complexes, there is a similar trend. For **8a−c**, the $^1J_{RhP}$ values range from 136.9 to 143.6 Hz, all of which are greater than the $^1J_{RhP}$ values for **6a−c** and **7a−c**.

It is known that phosphines with larger cone angles have smaller changes in ^{31}P NMR shift upon coordination to rhodium.[23] The differences in ^{31}P chemical shifts between **1a−c** and their rhodium complexes **6a−c** are δ 52.2, 54.7, and 56.1, respectively, which are consistent with a cone angle of approximately 110°. This trend of increasing shift with increasing donor ability is reversed for the pair of **2a−c** and **7a−c**; these differences in shifts are δ 83.7, 81.3, and 80.1, respectively. The significantly larger coordination shift relative to **1a−c** can be attributed to the smaller cone angle for this phosphine donor. The differences in ^{31}P chemical shift for **3a−c** and **8a−c** are δ 74.3, 68.1, and 67.8, respectively, which reflects the fact that phosphines **3a−c** have slightly larger cone angles than their Ti analogues but still smaller than **1a−c**.

Calculations. From the spectroscopic data, the role of the chelated metals on the electronic properties of the phosphine donors is clear but the mechanism by which the metal affects the donor properties is not. A simple hypothesis would be that the increase in C−P−C angle required to coordinate a transition metal would render these stronger σ-donors, as the lone pairs would possess less s-orbital character. Additionally, the increased negative charge on the amido donors in complexes **2a−c** and **3a−c** relative to **1a−c** would be expected to render the ligands containing a chelated early transition metal more strongly electron donating. Only an increase in the stability of the amido lone pair by π-back-donation to the early transition metal center could conceivably render the phosphine a weaker donor relative to **1a−c**.

There is a similarity of the complexes studied herein to compounds such as diazabicyclo[2,2,2]octane (N(CH₂-CH₂)₃N), where it was noted that there is little through-space overlap of the orbitals on nitrogen but enough through-bond

(23) Shaw, B. L.; Mann, B. E.; Masters, C. *J. Chem. Soc. A* **1971**, 1104−1106.
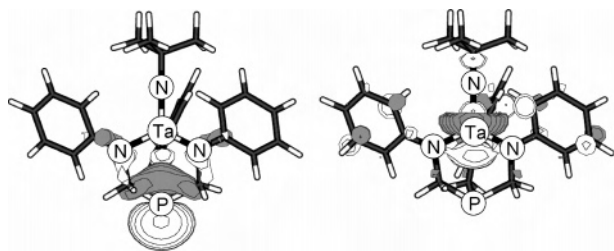
Figure 8. Depiction of the phosphorus lone pair orbital, HOMO-8, and Ta d_z orbital, LUMO+2 for complex **3b**, as determined by DFT using the B3LYP functional and LANL2DZ basis functions.

interactions to render the in-phase and out-of-phase combination of lone-pair orbitals on nitrogen different energies.[24] It is interesting to note that in the radical cation of diazabicyclo-[2,2,2]octane, $(N(CH_2CH_2)_3N)^{\bullet+}$, the ESR spectrum is indicative of a symmetric species, with equal coupling to two ^{14}N nuclei; however; it is unclear if this is delocalization is due to spatial overlap of the nitrogen orbitals or to rapid electron transfer through the ethylene bridge carbons.[25] The separation of the nitrogen atoms in diazabicyclo[2,2,2]octane complexes is typically around 2.6 Å, which is only ~0.4 Å shorter than the Ti···P and Ta···P distances observed here, and the significantly larger radii of both these transition metals and the phosphorus nuclei compared to nitrogen could allow for a direct through-space interaction.[9] Such an interaction could involve the overlap of a metal-based orbital with the minor lobe of the orbital associated with the lone pair. Alternatively, a net stabilization of the phosphine-based lone pair could occur by simple electrostatic interaction, providing a significant amount of electron density in the lone pair orbital resided close to the positively charged early transition metal center. With larger C−P−C angles increased p-orbital contribution to the lone pair orbital is anticipated, which should increase the relative magnitude of the minor lobe in this orbital. There is precedent for interactions of the minor lobe of a phosphine donor with a proximal transition metal center in the lowering of the inversion barrier for a phosphine.[26]

A DFT calculation was performed on complex **3b**, constrained to C_3 symmetry, using the B3LYP functional and the LANL2DZ basis function set provided in Gaussian 03. This level of theory overestimates the P···Ta distance by approximately 0.1 Å but otherwise adequately reproduces the crystallographically observed bond lengths and angles. A depiction of the HOMO-8, which is the orbital with the largest contribution from the lone pair on phosphorus, is shown in Figure 8. A natural bond order analysis determined the phosphorus lone pair to be of 50.03% p-orbital and 49.97% s-orbital character, which is reasonably close to that expected for the calculated C−P−C bond angle of 103°.[27]

The minor lobe of this orbital clearly extends back close to the tantalum center; however, there is no large contribution from the metal center in this orbital; any stabilization of the lone-pair orbital via direct through-space interaction must be largely electrostatic. An electrostatic stabilization of the phosphine lone pair would explain why the Ta(V) complexes are poorer donors than the Ti(IV) complexes. The reason for the lack of contribution from a tantalum-based orbital is not the lack of an orbital of appropriate symmetry but rather the energy difference between the metal-based orbital and the lone pair. The appropriate orbital is the LUMO+2 and is shown in Figure 8. This metal-based orbital extends considerably toward the phosphorus nucleus, and it is conceivable that by using a different transition metal fragment in the amido chelate a through-space covalent interactions between the transition metal and phosphine donor could be observed.

Conclusions. Ligands of the type $P(CH_2NAr^R)_3$ readily bind early transition metals using the amido donor, while retaining a phosphorus donor to bind to late transition metals, which allows for the facile syntheses of early−late heterobimetallics. The ^{31}P NMR shifts upon coordination of an early transition metal to the amido donors are opposite to the typical trend of increasing chemical shift with increasing C−P−C angle, and interactions with the transition metal d orbitals are likely the cause of these unusual ^{31}P NMR chemical shifts.

These are atypical phosphine donors, by virtue of the strained C−P−C angles required to chelate the early transition metals, as well as due to direct interactions between the early transition metal and the phosphine donor. The donor abilities of the titanium complexes are similar to those of the ubiquitous triphenylphosphine, but these are an unusual set of donors because their cone angles are similar to only the smallest trialkyl phosphines.[18,28]

Experimental Section

General Procedures. Unless otherwise stated, all manipulations were performed under an inert atmosphere of nitrogen using either standard Schlenk techniques or an MBraun glovebox. Dry, oxygen-free solvents were employed throughout. Anhydrous pentane, toluene, diethyl ether, and THF were purchased from Aldrich, sparged with dinitrogen, and passed through activated alumina under a positive pressure of nitrogen gas; toluene and hexanes were further deoxygenated using Ridox catalyst columns.[29] Deuterated benzene was dried by heating at reflux with sodium/potassium alloy in a sealed vessel under partial pressure, then trap-to-trap distilled, and freeze−pump−thaw degassed three times. Deuterated methylene chloride was heated in a sealed vessel over CaH_2, then trap-to-trap distilled, and freeze−pump−thaw degassed three times. NMR spectra were recorded on Bruker AMX (300 MHz) or Bruker AMX (500 MHz) spectrometer. All chemical shifts are reported in ppm, and all coupling constants are in Hz. For $^{19}F\{^1H\}$ NMR spectra, trifluoroacetic acid was used as the external reference at 0.00 ppm. ^{1}H NMR spectra were referenced to residual protons (C_6D_5H, δ 7.15; C_7D_7H, δ 2.09) with respect to tetramethylsilane at δ 0.00.

(24) Takahashi, M.; Matsuo, M.; Udagawa, Y. *Chem. Phys. Lett.* **1999**, *308*, 195−198. Nelsen, S. F.; Buschek, J. M. *J. Am. Chem. Soc.* **1974**, *96*, 7930−7933. Heilbronner, E.; Muszkat, K. A. *J. Am. Chem. Soc.* **1970**, *92*, 3818−3821.

(25) McKinney, T. M.; Geske, D. H. *J. Am. Chem. Soc.* **1965**, *87*, 3013−3014.

(26) Fryzuk, M. D.; Giesbrecht, G. R.; Rettig, S. J. *Inorg. Chem.* **1998**, *37*, 6928−6934.

(27) Nixon, J. F.; Pidcock, A. *Annu Rev. NMR Spectrosc.* **1969**, *2*, 345−422.

(28) Fey, N.; Tsipis, A. C.; Harris, S. E.; Harvey, J. N.; Orpen, A. G.; Mansson, R. A. *Chem. Eur. J.* **2005**, *12*, 291−302.

(29) Pangborn, A. B.; Giardello, M. A.; Grubbs, R. H.; Rosen, R. K.; Timmers, F. J. *Organometallics* **1996**, *15*, 1518−1520.

^{31}P{^{1}H} NMR spectra were referenced to external 85% H$_3$PO$_4$ at δ 0.0. ^{13}C{^{1}H} spectra were referenced relative to solvent resonances (C$_6$D$_6$, δ 128.0; C$_7$D$_8$, δ 20.4). Elemental analyses were performed by the Centre for Catalysis and Materials Research (CCMR), Windsor, Ontario, Canada. The compounds tris(hydroxylmethyl)phosphine, aniline, 3,5-dimethylaniline, 3,5-bis(trifluoromethyl)aniline, Ni(CO)$_4$, TiCl$_4$, LiNMe$_2$, Ta(NEt$_3$)$_2$(N^{t}Bu), and [(CO)$_2$Rh(μ-Cl)]$_2$ were purchased from Aldrich and used as received. The complex Ti(NMe$_2$)$_4$ was prepared from the reaction of TiCl$_4$ and LiNMe$_2$ and distilled prior to use.[30] Nickel tetracarbonyl, Ni(CO)$_4$, is highly toxic and should be handled with care.

P[CH$_2$NH-3,5-(CF$_3$)$_2$C$_6$H$_3$]$_3$ (1a). A mixture of P(CH$_2$OH)$_3$ (5.0 g, 90%, 0.0362 mol), 3,5-bis(trifluoromethyl)aniline (28 mL, 41.5 g, 5 equiv), and toluene (60 mL) were mixed in a 250 mL three-neck flask equipped with a Dean−Stark trap and a condenser. The solution was heated to reflux for 30 min, and the water was collected and removed from the trap. The solution was allowed to cool, and then the remaining solvent was removed under vacuum. The addition of pentane (80 mL) dissolved the excess 3,5-bis(trifluoromethyl)aniline and precipitated the product as a fine white solid, which was collected by filtration and dried under vacuum. X-ray-quality crystals were obtained from slow evaporation of the toluene solution. Yield 20.2 g, 73%. ^{1}H NMR (C$_6$D$_6$, 300 MHz, 298 K): δ 2.55 (dd, ^{3}J$_{HH}$ = 5.2 Hz, ^{2}J$_{PH}$ = 5.2 Hz, 6H, PCH$_2$), 3.13 (b, 3H, NH), 6.59 (s, 6H, Ph *o*-H), 7.27 (s, 3H, Ph *p*-H). ^{13}C{^{1}H} NMR (C$_6$D$_6$, 125.8 MHz, 298 K): δ 39.4 (d, J$_{PC}$ = 12.2 Hz, PCH$_2$), 111.2 and 122.1 (s, Ph *o*-C and *m*-C), 112.5. (s, Ph *p*-C), 132.9 (q, J = 32.9 Hz, Ph*C*-F$_3$), 148.9 (d, J = 5.5 Hz, *ipso*-C). ^{31}P{^{1}H} NMR (C$_6$D$_6$, 121.5 MHz, 298 K): δ −32.6 (s). ^{19}F{^{1}H} NMR (C$_6$D$_6$, 282.1 MHz, 298 K): δ 14.71 (s). Anal. Calcd for C$_{27}$H$_{18}$F$_{18}$N$_3$P: fw 757.10. C, 42.82; H, 2.40; N, 5.55. Found: C, 43.00; H, 2.49 N, 5.41.

P(CH$_2$NHPh)$_3$ (1b).[10] A mixture of P(CH$_2$OH)$_3$ (7.5 g, 0.0605 mol) and aniline (16.5 mL, 3 equiv) were stirred under dynamic vacuum. The solution became warm after 1 min and was then cooled after 10 min. Shortly thereafter, the mixture solidified and was left under vacuum for 2 h. The addition of ether to the mixture and filtering the resulting solid removed any trace remaining aniline. The sample was crystallized by cooling a warm saturated toluene solution sample at −40 °C. The white solid was filtered, rinsed with pentane, and dried (15.8 g, 75%). ^{1}H NMR (C$_6$D$_6$, 300 MHz, 298 K): δ 3.23 (d, ^{2}J$_{PH}$ = 4.8 Hz, 6H, PCH$_2$), 3.47 (b, 3H, NH), 6.48 (dd, 6H, Ph *o*-H), 6.76 (t, 3H, Ph *p*-H), 7.16 (m, Ph *m*-H). ^{13}C{^{1}H} NMR (C$_6$D$_6$, 125.8 MHz, 298 K): δ 40.6 (d, J$_{PC}$ = 12.5 Hz, PCH$_2$), 113.2 and 118.2 (s, Ph *o*-C and *m*-C), 117.0. (s, Ph *p*-C), 148.5 (d, J = 4.5 Hz, *ipso*-C). ^{31}P{^{1}H} NMR (C$_6$D$_6$, 121.5 MHz, 298 K): δ −32.1 (s). Anal. Calcd for C$_{21}$H$_{24}$N$_3$P: fw 349.41. C, 72.19; H, 6.92; N, 12.03. Found: C, 72.55; H, 7.00 N, 11.64.

P(CH$_2$NH-3,5-Me$_2$C$_6$H$_3$)$_3$ (1c). The mixture of P(CH$_2$OH)$_3$ (17.36 g, 0.126 mol) and 3,5-dimethylaniline (45.8 g, 3 equiv) was stirred under dynamic vacuum. The solution became warm after 1 min and was then cooled after 10 min. Shortly thereafter, the mixture solidified. Residual 3,5-dimethylaniline was removed by adding pentane to the mixture and filtering the resulting solid. The sample was crystallized by cooling a warm saturated toluene solution to −40 °C. The white solid was filtered, rinsed with pentane, and dried (42.7 g, 78%). ^{1}H NMR (C$_6$D$_6$, 300 MHz, 298 K): δ 2.18 (s, 18H, PhCH$_3$), 3.23 (d, ^{2}J$_{PH}$ = 5.2 Hz, 6H, PCH$_2$), 3.49 (b, 3H, NH), 6.23 (s, 6H, Ph *o*-H), 6.42 (s, 3H, Ph *p*-H). ^{13}C{^{1}H} NMR (C$_6$D$_6$, 125.8 MHz, 298 K): δ22.1 (s, Ph*C*H$_3$), 41.1

(d, J$_{PC}$ = 13.1 Hz, PCH$_2$), 112.2 and 120.9 (s, Ph *o*-C and *m*-C), 139.1 (s, Ph *p*-C), 149.3 (d, J = 4.8 Hz, *ipso*-C). ^{31}P{^{1}H} NMR (C$_6$D$_6$, 121.5 MHz, 298 K): δ −29.6 (s). Anal. Calcd for C$_{27}$H$_{36}$N$_3$P: fw 433.57; C, 74.80; H, 8.37; N, 9.69. Found: C, 74.50; H, 8.49 N, 9.40.

P(CH$_2$NAr^{CF_3})$_3$TiNMe$_2$ (2a). A solution of Ti(NMe$_2$)$_4$ (754.78 mg, 3.37 mmol) in toluene (60 mL) was added to a solution of **1a** (2.55 g, 3.37 mmol) in 50 mL of toluene. The pale yellow solution was stirred for 10 h and turned dark red. The solvent was removed under vacuum, and the remaining dark red solid was rinsed with a small portion of pentane and then dried under vacuum (2.45 g, 85%). X-ray-quality crystals were obtained by slow evaporation of a benzene solution. ^{1}H NMR (C$_6$D$_6$, 300 MHz, 298 K): δ 2.85 (s, 6H, NCH$_3$), 3.18 (d, 6H, ^{2}J$_{PH}$ = 7.0 Hz, PCH$_2$), 6.81 (s, 6H, Ph *o*-H), 7.40 (s, 3H, Ph *p*-H). ^{13}C{^{1}H} NMR (C$_6$D$_6$, 125.8 MHz, 298 K): δ 41.2 (s, TiNCH$_3$), 44.1 (d, J$_{PC}$ = 24.2 Hz, PCH$_2$), 113.4 and 122.1 (s, Ph *o*-C and *m*-C), 116.0 (s, Ph *p*-C), 132.6 (q, J = 32.9 Hz, Ph*C*-F$_3$), 152.9(d, *ipso*-C). ^{31}P{^{1}H} NMR (C$_6$D$_6$, 121.5 MHz, 298 K): δ −79.9 (s). ^{19}F{^{1}H} NMR (C$_6$D$_6$, 282.1 MHz, 298 K): δ 14.88 (s). Anal. Calcd for C$_{29}$H$_{21}$F$_{18}$N$_4$PTi, fw 846.32. C, 41.16; H, 2.50; N, 6.62. Found: C, 40.72; H, 2.70; N, 6.71.

P(CH$_2$NPh)$_3$TiNMe$_2$ (2b). Prepared in an analogous manner to **2a** from Ti(NMe$_2$)$_4$ (2.63 g, 11.73 mmol) and **1b** (4.09 g, 11.73 mmol) using a reaction time of 12 h. Yield 4.10 g (83%). ^{1}H NMR (C$_6$D$_6$, 500.1 MHz, 298 K): δ 2.98 (s, 6H, TiNMe$_2$), 3.84 (d, 6H, ^{2}J$_{PH}$ = 6.7 Hz, PCH$_2$), 6.72 (d, 6H, ^{3}J$_{HH}$ = 8.3 Hz, Ph *o*-H), 6.86 (t, 3H, Ph *p*-H), 7.20 (m, 6H, Ph *m*-H). ^{13}C{^{1}H} NMR (C$_6$D$_6$, 125.8 MHz, 298 K): δ 42.4 (s, TiNMe$_2$), 45.9 (d, J$_{PC}$ = 20.2 Hz, P*C*H$_2$), 117.7 and 129.7 (s, Ph *o*-Cand *m*-C), 120.9 (s, Ph *p*-C), 154.2 (m, *ipso*-C). ^{31}P{^{1}H} NMR (C$_6$D$_6$, 202.5 MHz, 298 K): δ −65.6 (s). Anal. Calcd for C$_{23}$H$_{27}$N$_4$PTi: fw 438.33. C, 63.02; H, 6.21; N, 12.78. Found: C, 63.24; H, 6.25 N, 12.44.

P(CH$_2$NAr^{Me})$_3$TiNMe$_2$ (2c). A solution of Ti(NMe$_2$)$_4$ (2.63 g, 11.73 mmol) in toluene (50 mL) was added to a solution of **1c** (5.08 g, 11.73 mmol) in 50 mL of toluene. The solution gradually turned dark red over 24 h. The solution was evaporated to dryness, and 5 mL of pentane and 10 mL of hexamethyldisiloxane were added. The solution was filtered, and the dark red solid dried under vacuum (5.62 g, 92%). X-ray-quality crystals were obtained from slow evaporation of a pentane solution. ^{1}H NMR (C$_6$D$_6$, 500 MHz, 298 K): δ 2.22 (s, 18H, ArCH$_3$), 3.15 (s, 6H, NMe$_2$), 3.95 (d, ^{2}J$_{PH}$ = 7.3 Hz, 6H, PCH$_2$), 6.49 (s, 6H, *o*-H), 6.53 (s, 3H, *p*-H). ^{13}C{^{1}H} NMR (C$_6$D$_6$, 125.8 MHz, 298 K): δ22.2 (s, ArCH$_3$), 42.8 (s, NMe$_2$), 46.3 (d, J$_{PC}$ = 19.9 Hz, PCH$_2$), 115.9, 122.7, and 138.7 (s, Ph *o*-C , *m*-C and *p*-C), 154.4 (d, ^{3}J = 1.6 Hz, *ipso*-C). ^{31}P{^{1}H} NMR (C$_6$D$_6$, 202.5 MHz, 298 K): δ −61.6 (s). Anal. Calcd for C$_{29}$H$_{39}$N$_4$PTi, fw 522.49. C, 66.66; H, 7.52; N, 10.72. Found: C, 67.02; H, 7.71; N, 11.01.

P(CH$_2$NAr^{CF_3})$_3$Ta═N^{t}Bu (3a). A solution of (Et$_2$N)$_3$Ta═N^{t}Bu (234.3 mg, 0.5 mmol) in 10 mL of toluene was added to a solution of **1b** (379 mg, 0.5 mmol) in 30 mL of toluene. The solution was stirred overnight. The solvent was removed under vacuum, and the remaining pale yellow solid was rinsed with a small portion of pentane and then dried under vacuum (315 mg, 60%). ^{1}H NMR (C$_6$D$_6$, 300 MHz, 298 K): δ 1.65 (s, 9H, Ta═NCMe$_3$), 3.10 (d, 6H, ^{2}J$_{PH}$ = 6.7 Hz, PCH$_2$), 7.15 (s, 3H, Ph *p*-H), 7.54 (s, 6H, Ph *o*-H). ^{13}C{^{1}H} NMR (C$_6$D$_6$, 125.8 MHz, 298 K): δ 32.6 (s, 9H, Ta═NCMe$_3$), 41.8 (d, J$_{PC}$ = 30.1 Hz, PCH$_2$), 70.4 (s, Ta═NCMe$_3$), 118.4 and 129.6 (s, Ph *o*-C and *m*-C), 125.9 (s, Ph *p*-C), 132.8 (q, J = 32.9 Hz, Ph*C*-F$_3$), 152.5(s, *ipso*-C). ^{31}P{^{1}H} NMR (C$_6$D$_6$, 121.5 MHz, 298 K): δ −108.5 (s). ^{19}F{^{1}H} NMR (C$_6$D$_6$, 282.1 MHz, 298 K): δ 14.2 (s). Anal. Calcd for

(30) Diamond, G. M.; Jordan, R. F.; Petersen, J. L. *Organometallics* **1996**, *15*, 4030−4037.

$C_{31}H_{24}F_{18}N_4PTa\cdot(0.5\ C_7H_8)$: C, 39.34; H, 2.7; N, 5.32. Found: C, 39.71; H, 3.30; N, 5.29.

P(CH₂NPh)₃Ta=N'Bu (3b). Prepared in an analogous manner to **3a** using (Et₂N)₃Ta=N'Bu (234.3 mg, 0.5 mmol) and **1b** (173 mg, 0.5 mmol). Yield 389 mg (65%). ¹H NMR (C₆D₆, 500.1 MHz, 298 K): δ 1.62 (s, 9H, Ta=NC**Me**₃), 3.67 (d, 6H, $^2J_{PH}$ = 7.3 Hz, PC**H**₂), 6.90 (t, 6H, $^3J_{HH}$ = 7.3 Hz, Ph o-**H**), 7.27 (t, 3H, $^3J_{HH}$ = 7.8 Hz, Ph p-**H**), 7.40 (m, 6H, Ph m-**H**). ¹³C{¹H} NMR (C₆D₆, 125.8 MHz, 298 K): δ 33.8 (s, Ta=NC**Me**₃), 42.6 (d, J_{PC} = 26.8 Hz, P**C**H₂), 69.1 (s, Ta=N**C**Me₃), 119.1 and 129.1 (s, Ph o-**C** and m-**C**), 121.5 (s, Ph p-**C**), 152.3 (s, ipso-**C**). ³¹P{¹H} NMR (C₆D₆, 202.5 MHz, 298 K): δ −100.9 (s). Anal. Calcd for $C_{25}H_{30}N_4PTa$: fw 598.45. C, 50.17; H, 5.05; N, 9.36. Found: C, 50.65; H, 5.25; N, 9.01.

P(CH₂NAr^Me)₃Ta=N'Bu (3c). Prepared in an analogous manner to **3a** using (Et₂N)₃Ta=N'Bu (234.3 mg, 0.5 mmol) and **1c** (215 mg, 0.5 mmol) and a reaction time of 72 h. Yield 204.6 mg (60%). X-ray-quality crystals were obtained from slow evaporation of the benzene solution. ¹H NMR (C₆D₆, 300 MHz, 298 K): δ 1.71 (s, 9H, Ta=NC**Me**₃), 2.32 (s, 18H, ArC**H**₃), 3.73 (d, $^2J_{PH}$ = 6.7 Hz, 6H, PC**H**₂), 6.61 (s, 6H, o-**H**), 7.11 (s, 3H, p-**H**). ¹³C{¹H} NMR (C₆D₆, 125.8 MHz, 298 K): δ21.9 (s, Ar**C**H₃), 33.6 (s, 9H, Ta=N**C**Me₃), 42.7 (d, J_{PC} =26.3 Hz, N**Me**₂), 68.9 (s, Ta=N**C**Me₃), 116.2 (s, Ph o-**C**), 117.9 (s, Ph m-**C**), 138.7 (s, Ph p-**C**), 152.5(s, ipso-**C**). ³¹P{¹H} NMR (C₆D₆, 202.5 MHz, 298 K): δ −100.1 (s). Anal. Calcd for $C_{31}H_{42}N_4PTa$: fw 682.61. C, 54.55; H, 6.20; N, 8.21. Found: C, 54.07; H, 6.11; N, 8.77.

(CO)₃Ni(PCH₂NAr^Me)₃TiNMe₂ (4). Excess Ni(CO)₄ was vacuum-transferred onto a solution of **2c** (1.25 g, 2.87 mmol) in 50 mL of toluene. The dark red solution was stirred 5 min and then evaporated to dryness to provide a dark red product (1.77 g, 93%). The product was stable for short durations in CH₂Cl₂, as judged by ³¹P{¹H} NMR spectroscopy, and the IR spectrum of a 0.05 M solution was obtained in this solvent. Solutions kept at room temperature are not stable and gradually undergo ligand redistribution with loss of Ni(CO)₄ and thus should be handled with care. ¹H NMR (C₆D₆, 500 MHz, 298 K): δ 2.17 (s, 18H, ArC**H**₃), 3.06 (s, 6H, N**Me**₂), 4.07 (s, 6H, PC**H**₂), 6.46 (s, 6H, o-**H**), 6.52 (s, 3H, p-**H**). ¹³C{¹H} NMR (C₆D₆, 125.8 MHz, 298 K): δ22.0 (s, Ar**C**H₃), 42.9 (s, N**Me**₂), 52.5 (d, J_{PC} = 15.5 Hz, P**C**H₂), 116.1, 123.6, and 139.1 (s, Ph o-**C**, m-**C** and p-**C**), 153.8 (d, $^3J_{PC}$ = 6.9 Hz, ipso-**C**), 196.3 (d, $^2J_{PC}$ = 1.1 Hz, Ni(**C**O)₃). ³¹P{¹H} NMR (C₆D₆, 202.5 MHz, 298 K): δ 4.1 (s). Anal. Calcd for $C_{32}H_{39}N_4O_3PTi$: fw 665.21; C, 57.78; H, 5.91; N, 8.42. Found: C, 58.01; H, 5.94; N, 8.39. IR: (CH₂Cl₂, 0.05M) 2073.7 cm⁻¹ (s, A_1), 2041.0 cm⁻¹ (w), 2000.0 cm⁻¹ (br, E).

(CO)₂Ni[P(CH₂NAr^Me)₃TiNMe₂]₂ (5). Solid **1c** (482.8 mg, 0.924 mmol) was added to a solution of **4** (614.9 mg, 0.924 mmol) in 50 mL of toluene. The solution was stirred for 48 h and evaporated to dryness, and 15 mL of pentane was added. The solution was filtered and the remaining dark red solid was rinsed with a small portion of pentane and then dried under vacuum. The complex is slightly soluble in pentane, and X-ray crystals were obtained by cooling a pentane solution to −40 °C. ¹H NMR (C₆D₆, 500 MHz, 298 K): δ 2.17 (s, 18H, ArC**H**₃), 3.06 (s, 6H, N**Me**₂), ¹H NMR (C₆D₆, 500 MHz, 298 K): δ 2.15 (s, 18H, ArC**H**₃), 3.12 (s, 6H, N**Me**₂), 4.37 (s, 6H, PC**H**₂), 6.51 (s, 3H, p-**H**), 6.56 (s, 6H, o-**H**). ¹³C{¹H} NMR (C₆D₆, 125.8 MHz, 298 K): δ 22.0 (s, Ar**C**H₃), 42.9 (s, N**Me**₂), 54.0 (vt, J_{PC} = 15.5 Hz, P**C**H₂), 116.0, 123.4, and 139.0 (s, Ph o-**C**, m-**C** and p-**C**), 153.8 (d, $^3J_{PC}$ = 6.9 Hz, ipso-**C**), 190.0 (t, $^2J_{PC}$ = 1.1 Hz, Ni(**C**O)₃). ³¹P{¹H} NMR (C₆D₆, 202.5 MHz, 298 K): δ 7.03 (s). Anal. Calcd for $C_{60}H_{78}N_8NiO_2P2Ti_2$: fw 1159.69; C, 62.14; H, 6.78; N, 9.66. Found: C, 62.33; H, 6.96; N, 9.47.

trans-RhCl(CO)(1a)₂ (6a). A solution of **1a** (60.8 mg, 0.08 mmol) in 0.4 mL of CD₂Cl₂ was added to [RhCl(CO)₂]₂ (7.8 mg, 0.02 mmol) in 0.4 mL of CD₂Cl₂. Gas evolution was observed, and the solution turned dark orange over the course of 20 min. ¹H NMR (CD₂Cl₂, 300 MHz, 298 K): δ 3.1 (s, 6H, PC**H**₂), 4.82 (s, 3H, N**H**), 7.05 (s, 6H, Ph o-**H**), 7.24 (s, 3H, Ph p-**H**). ¹³C{¹H} NMR (CD₂Cl₂, 125.8 MHz, 298 K): δ 39.1 (s, P**C**H₂), 112.8 (s, **C**O), 113.2 and 122.1 (s, Ph o-**C** and m-**C**), 118.5 (s, Ph p-**C**), 132.9 (q, J = 33.1 Hz, Ph**C**-F₃), 148.9 (s, ipso-**C**). ³¹P{¹H} NMR (CD₂Cl₂, 121.5 MHz, 298 K): δ 22.6 (d, J_{PRh} = 120.1 Hz). ¹⁹F-{¹H} NMR (CD₂Cl₂, 282.1 MHz, 298 K): δ 14.00 (s). IR: 1984.9 cm⁻¹.

trans-RhCl(CO)(1b)₂ (6b). A solution of 28.0 mg (0.08 mmol) of **1b** in 0.4 mL of CD₂Cl₂ was added to [RhCl(CO)₂]₂ (7.8 mg, 0.02 mmol) in 0.4 mL of CD₂Cl₂. ¹H NMR (CD₂Cl₂, 300.1 MHz, 298 K): δ 3.95 (s, 6H, PC**H**₂), 4.28 (b, 3H, N**H**), 6.78 (m, 6H, Ph o-**H**), 7.20 (t, 3H, Ph p-**H**), 7.35 (s, 6H, Ph m-**H**). ¹³C{¹H} NMR (CD₂Cl₂, 125.8 MHz, 298 K): δ 39.7 (t, J_{PC} = 14.5 Hz, P**C**H₂), 114.2 (s, **C**O), 119.3 and 129.9 (s, Ph o-**C** and m-**C**), 128.8 (s, Ph p-**C**), 148.2 (m, ipso-**C**). ³¹P{¹H} NMR (CD₂Cl₂, 202.5 MHz, 298 K): δ 23.7 (d, J_{PRh} = 118.1 Hz). IR: 1976.3 cm⁻¹.

trans-RhCl(CO)(1c)₂ (6c). A solution of **1c** (34.4 mg, 0.08 mmol) in 0.4 mL of CD₂Cl₂ was added to[RhCl(CO)₂]₂ (7.8 mg, 0.02 mmol) in 0.4 mL of CD₂Cl₂. ¹H NMR (CD₂Cl₂, 300 MHz, 298 K): δ 2.20 (s, 18H, Ph C**H**₃), 3.93 (s, 6H, PC**H**₂), 4.24 (b, 3H, N**H**), 6.32 (s, 6H, Ph o-**H**), 6.43 (s, 3H, Ph p-**H**). ¹³C{¹H} NMR (CD₂Cl₂, 125.8 MHz, 298 K): δ21.7 (s, Ph**C**H₃), 39.6 (t, J_{PC} = 13.4 Hz, P**C**H₂), 116.0 (s, **C**O), 112.0 and 121.2 (s, Ph o-**C** and m-**C**), 139.6 (s, Ph p-**C**), 148.3 (t, ipso-**C**). ³¹P{¹H} NMR (CD₂Cl₂, 121.5 MHz, 298 K): δ 23.5 (d, J_{PRh} = 116.9 Hz). IR: 1973.2 cm⁻¹.

trans-RhCl(CO)(2a)₂ (7a). A solution of **2a** (64.1 mg, 0.08 mmol) in 0.4 mL of CD₂Cl₂ was added to [RhCl(CO)₂]₂ (7.8 mg, 0.02 mmol) in 0.4 mL of CD₂Cl₂. ¹H NMR (CD₂Cl₂, 300 MHz, 298 K): δ 3.5 (s, 6H, NC**H**₃), 4.8 (s, PC**H**₂), 7.29 (s, 6H, Ph o-**H**), 7.54 (s, 3H, Ph p-**H**). ¹³C{¹H} NMR (CD₂Cl₂, 125.8 MHz, 298 K): δ 42.7 (s, TiN**C**H₃), 49.3 (s, P**C**H₂), 115.2 (s, **C**O), 113.4 and 122.1 (s, Ph o-**C** and m-**C**), 117.3 (s, Ph p-**C**), 133.1 (q, J = 32.8 Hz, Ph**C**-F₃), 153.2(s, ipso-**C**). ³¹P{¹H} NMR (CD₂Cl₂, 121.5 MHz, 298 K): δ 3.8 (d, J_{PRh} = 130.3 Hz). ¹⁹F{¹H} NMR (CD₂Cl₂, 282.1 MHz, 298 K): δ 14.3 (s). IR: 1988.1 cm⁻¹.

trans-RhCl(CO)(2b)₂ (7b). A solution of **2b** (35.2 mg, 0.08 mmol) in 0.4 mL of CD₂Cl₂ was added to 7.8 mg (0.02 mmol) of [RhCl(CO)₂]₂ in 0.4 mL of CD₂Cl₂. ¹H NMR (CD₂Cl₂, 300 MHz, 298 K): δ 3.3 (s, 6H, TiN**Me**₂), 4.6 (s, PC**H**₂), 6.82 (d, 6H, $^3J_{HH}$ = 7.8 Hz, Ph o-**H**), 6.89 (t, 3H, Ph p-**H**), 7.30 (t, 6H, Ph m-**H**). ¹³C{¹H} NMR (CD₂Cl₂, 125.8 MHz, 298 K): δ 43.0 (s, TiN**Me**₂), 49.7 (s, P**C**H₂), 117.5 (s, **C**O), 117.7 and 129.7 (s, Ph o-**C** and m-**C**), 121.6 (s, Ph p-**C**), 153.5 (m, ipso-**C**). ³¹P{¹H} NMR (CD₂Cl₂, 202.5 MHz, 298 K): δ 15.7 (d, J_{PRh} = 125.8 Hz). IR: 1979.6 cm⁻¹.

trans-RhCl(CO)(2c)₂ (7c). A solution of **2c** (42.0 mg, 0.08 mmol) in 0.4 mL of CD₂Cl₂ was added to [RhCl(CO)₂]₂ (7.8 mg, 0.02 mmol) in 0.4 mL of CD₂Cl₂. ¹H NMR (CD₂Cl₂, 300 MHz, 298 K): δ 2.28 (s, 18H, ArC**H**₃), 3.26 (s, 6H, N**Me**₂), 4.56(s, 6H, PC**H**₂), 6.46 (s, 6H, o-**H**), 6.47 (s, 3H, p-**H**). ¹³C{¹H} NMR (CD₂Cl₂, 125.8 MHz, 298 K): δ21.9 (s, Ar**C**H₃), 43.3 (s, N**Me**₂), 49.6-(s, P**C**H₂), 112.1 (s, **C**O), 115.6, 123.2, and 139.2 (s, Ph o-**C**, m-**C** and p-**C**), 153.5 (s, ipso-**C**). ³¹P{¹H} NMR (CD₂Cl₂, 202.5 MHz, 298 K): δ 18.51 (d, J_{PRh} = 122.5 Hz). IR: 1974.8 cm⁻¹.

trans-RhCl(CO)(3a)₂ (8a). A solution of **3a** (80.5 mg, 0.08 mmol) in 0.4 mL of CD₂Cl₂ was added to 7.8 mg (0.02 mmol) of [RhCl(CO)₂]₂ in 0.4 mL of CD₂Cl₂. ¹H NMR (CD₂Cl₂, 300 MHz, 298 K): δ 1.59 (s, 9H, Ta=NC**Me**₃), 4.90 (s, PC**H**₂), 7.55 (s, 3H,

Ph *p*-**H**), 7.82 (s, 6H, Ph *o*-**H**). $^{13}C\{^{1}H\}$ NMR (CD_2Cl_2, 125.8 MHz, 298 K): δ 32.9 (s, 9H, Ta=NC**Me**$_3$), 53.3 (d, J_{PC} = 30.1 Hz, P**CH**$_2$), 72.2 (s, Ta=N**C**Me$_3$), 116.2 and 129.6 (s, Ph *o*-**C** and *m*-**C**), 125.9 (s, Ph *p*-**C**), 132.8 (q, *J* = 33.2 Hz, Ph**C**-F$_3$), 152.8(t, *ipso*-**C**). $^{31}P\{^{1}H\}$ NMR (CD_2Cl_2, 121.5 MHz, 298 K): δ −34.2 (d, J_{PRh} = 143.6 Hz). $^{19}F\{^{1}H\}$ NMR (CD_2Cl_2, 282.1 MHz, 298 K): δ 14.9 (s). IR: 1990.5 cm^{-1}.

trans-**RhCl(CO)(3b)$_2$ (8b).** A solution of **3b** (48.0 mg, 0.08 mmol) in 0.4 mL of CD_2Cl_2 was added to[RhCl(CO)$_2$]$_2$ (7.8 mg, 0.02 mmol) in 0.4 mL of CD_2Cl_2. ^{1}H NMR (CD_2Cl_2, 300.1 MHz, 298 K): δ 1.59 (s, 9H, Ta=NC**Me**$_3$), 4.82 (s, P**CH**$_2$), 6.95 (t, 6H, $^{3}J_{HH}$ = 7.3 Hz, Ph *o*-**H**), 7.3 (t, 3H, $^{3}J_{HH}$ = 7.8 Hz, Ph *p*-**H**), 7.44 (d, 6H, Ph *m*-**H**). $^{13}C\{^{1}H\}$ NMR (CD_2Cl_2, 125.8 MHz, 298 K): δ 32.9 (s, Ta=NC**Me**$_3$), 46.7 (s, P**CH**$_2$), 69.8 (s, Ta=N**C**Me$_3$), 117.7 (s, **C**O), 118.4 and 128.5(s, Ph *o*-C and *m*-**C**), 121.3 (s, Ph *p*-**C**), 151.0 (s, *ipso*-**C**). $^{31}P\{^{1}H\}$ NMR (CD_2Cl_2, 202.5 MHz, 298 K): δ −32.8 (d, J_{PRh} = 138.11 Hz). IR: 1986.7 cm^{-1}.

trans-**RhCl(CO)(3c)$_2$ (8c).** A solution of **3c** (54.6 mg, 0.08 mmol) in 0.4 mL of CD_2Cl_2 was added to 7.8 mg (0.02 mmol) of [RhCl(CO)$_2$]$_2$ in 0.4 mL of CD_2Cl_2. X-ray-quality crystals were obtained from slow evaporation of the CD_2Cl_2 solution at −40 °C. ^{1}H NMR (CD_2Cl_2, 300 MHz, 298 K): δ 1.63 (s, 9H, Ta=NC**Me**$_3$), 2.32 (s, 18H, ArC**H**$_3$), 4.77 (s, 6H, P**CH**$_2$), 6.61 (s, 6H, *o*-**H**), 7.08 (s, 3H, *p*-**H**). $^{13}C\{^{1}H\}$ NMR (CD_2Cl_2, 125.8 MHz, 298 K): δ21.7 (s, Ar**C**H$_3$), 33.5 (s, Ta=NC**Me**$_3$), 47.4 (s, N**Me**$_2$), 70.4 (s, Ta=N**C**Me$_3$), 116.3 (s, **C**O), 116.9 (s, Ph *o*-**C**), 123.9 (s, Ph *m*-**C**), 138.9 (s, Ph *p*-**C**), 151.9 (s, *ipso*-**C**). $^{31}P\{^{1}H\}$ NMR (CD_2Cl_2, 202.5 MHz, 298 K): δ −32.3 (d, J_{PRh} = 136.9 Hz). IR: 1986.6 cm^{-1}. Anal. Calcd for $C_{63}H_{84}N_8OClP_2Ta_2$: C, 49.40; H, 5.53; N, 7.32. Found: C, 49.09; H, 5.64; N, 7.27.

X-ray Crystallography. The X-ray structures were obtained at low temperature, with each crystal covered in Paratone and placed rapidly into the cold N$_2$ stream of the Kryo-Flex low-temperature device. The data were collected using the SMART[31] software on a Bruker APEX CCD diffractometer using a graphite monochromator with Mo Kα radiation (λ = 0.71073 Å). A hemisphere of data was collected using a counting time of 10−30 s per frame. Details of crystal data, data collection, and structure refinement are listed in Table 1. Data reductions were performed using the SAINT[32] software, and the data were corrected for absorption using SAD-ABS.[33] The structures were solved by direct methods using SIR97[34] and refined by full-matrix least-squares on F^2 with anisotropic displacement parameters for the non-H atoms using SHELXL-97[35]

and the WinGX[36] software package, and thermal ellipsoid plots were produced using ORTEP32.[37] The thermal parameters for the carbonyl fragment in **8c** were modeled isotropically due to problems arising from its 3-fold disorder.

Calculations. Ab initio DFT calculations were performed using the hybrid functional B3LYP[38] method with the Gaussian 03 package.[39] The basis functions used were the LANL2DZ set, provided in the Gaussian 03 program.

Supporting Information Available: Crystallographic data in the form of cif files for **1c**, **2b**, **3c**, **5**, and **8c**; energy and optimized geometry coordinates for DFT calculation on **3b** and crystallographic data. This material is available free of charge via the Internet at http://pubs.acs.org.

IC060692D

(31) *SMART, Molecular analysis research tool*; Bruker AXS, Inc.: Madison, WI, 2001.
(32) *SAINTPlus, Data reduction and correction program*; Bruker AXS, Inc.: Madison, WI, 2001.
(33) *SADABS, An empirical absorption correction program*; Bruker AXS, Inc.: Madison, WI, 2001.
(34) Altomare, A.; Burla, M. C.; Camalli, M.; Cascarano, G. L.; Giacovazzo, C.; Guagliardi, A.; Moliterni, A. G. G.; Polidori, G.; Spagna, R. *J. Appl. Crystallogr.* **1999**, *32*, 115−119.
(35) Sheldrick, G. M. *SHELXL-97*; Universitat Göttingen: Göttingen, Germany, 1997.
(36) Farrugia, L. *J. Appl. Crystallogr.* **1999**, *32*, 837−838.
(37) Farrugia, L. *J. Appl. Crystallogr.* **1997**, *30*, 565.
(38) Becke, A. D. *J. Chem. Phys.* **1993**, *98*, 5648−5652.
(39) Frisch, M. J.; Trucks, G. W.; Schlegel, H. B.; Scuseria, G. E.; Robb, M. A.; Cheeseman, J. R.; Montgomery, J. A., Jr.; Vreven, T.; Kudin, K. N.; Burant, J. C.; Millam, J. M.; Iyengar, S. S.; Tomasi, J.; Barone, V.; Mennucci, B.; Cossi, M.; Scalmani, G.; Rega, N.; Petersson, G. A.; Nakatsuji, H.; Hada, M.; Ehara, M.; Toyota, K.; Fukuda, R.; Hasegawa, J.; Ishida, M.; Nakajima, T.; Honda, Y.; Kitao, O.; Nakai, H.; Klene, M.; Li, X.; Knox, J. E.; Hratchian, H. P.; Cross, J. B.; Bakken, V.; Adamo, C.; Jaramillo, J.; Gomperts, R.; Stratmann, R. E.; Yazyev, O.; Austin, A. J.; Cammi, R.; Pomelli, C.; Ochterski, J. W.; Ayala, P. Y.; Morokuma, K.; Voth, G. A.; Salvador, P.; Dannenberg, J. J.; Zakrzewski, V. G.; Dapprich, S.; Daniels, A. D.; Strain, M. C.; Farkas, O.; Malick, D. K.; Rabuck, A. D.; Raghavachari, K.; Foresman, J. B.; Ortiz, J. V.; Cui, Q.; Baboul, A. G.; Clifford, S.; Cioslowski, J.; Stefanov, B. B.; Liu, G.; Liashenko, A.; Piskorz, P.; Komaromi, I.; Martin, R. L.; Fox, D. J.; Keith, T.; Al-Laham, M. A.; Peng, C. Y.; Nanayakkara, A.; Challacombe, M.; Gill, P. M. W.; Johnson, B.; Chen, W.; Wong, M. W.; Gonzalez, C.; Pople, J. A. *Gaussian 03*, revision C.02; Gaussian, Inc.: Wallingford, CT, 2004.